Supplemental Material

Expanded Methods

Animals

Animal experiments were performed in accordance with the University of California Los Angeles (UCLA) Institutional Animal Care and Use Committee, and euthanasia protocols conform to the National Institutes of Health's Guide for the Care and Use of Laboratory Animals (2011). Data for all experiments were collected from 42 male and female Yucatán minipigs (> 3 months old).

Human Cardiac Specimens

Use of a fresh frozen cadaveric heart (Donated Body Program, UCLA) from a 97-year-old woman with history of coronary artery disease who died of cardiopulmonary failure was approved by the UCLA Institutional Review Board (**Online Table I**).

Three de-identified donor human hearts were approved for research by the Institutional Review Board (Office of Human Research) at the George Washington University. Human hearts were procured by Washington Regional Transplant Community and arrested in ice-cold cardioplegic solution in the operating room prior to delivery to GWU. An RAGP from a 31-year-old man with no cardiac history who died of anoxia (hanging) was immersion fixed in 4% paraformaldehyde (PFA) and used for histologic study. The specimen used for tissue clearing was from a 71-year-old Asian woman with history of diabetes mellitus and hypertension who died following a large intracranial hemorrhagic stroke. The heart used for optical mapping was from a 52-year-old Caucasian woman with history of hypertension and hyperlipidemia who died of stroke.

Perfusion Fixation of Human Heart

A de-identified female donor heart without underlying cardiac disease underwent perfusion fixation with 4% PFA for tissue clearing. Three of the pulmonary veins and the inferior vena cava were sutured closed with one pulmonary vein and the superior vena cava serving as outflow of perfusate. The aortic root and pulmonary artery were cannulated with 24 Fr cannulas. Perfusion of 4% PFA via these cannulas was performed at flow rates to distend of the cardiac chambers. Perfusion was maintained at 4°C for 24 hours. The cannulas and outflow were then clamped, and the tissue was immersion fixed with agitation at 4°C overnight. The heart was then washed with 0.01 mol/L phosphate-buffered saline (PBS) perfusate for 30 minutes via cannulas followed by three 0.01 mol/L PBS washes for 30 minutes. The heart was then stored in 0.01 mol/L PBS/0.02% sodium azide at 4°C until processing for modified immunolabeling-enabled three-Dimensional Imaging of Solvent-Cleared Organs (iDISCO+) tissue clearing.

Coronary Artery Contrast Injection and Imaging

The right side of the fresh frozen cadaveric human female cardiac specimen was used to determine the vascular supply of the right atrial ganglionated plexus (RAGP). The right coronary artery was selectively cannulated. BriteVu media (Scarlet Imaging) was prepared by heating diH_2O to 40-45°C. 700 µL of BriteVu enhancer was added to 105 mL of warmed water. After 1 minute, 35 g of BriteVu (40% wt/vol) was added to solution and heated to 70-80°C for 10 minutes with agitation. The solution was allowed to cool to 45°C and pressure perfused using a peristaltic pump (PERIPRO-4HS, World Precision

Instruments) into the right coronary artery at 50 mL/min. The specimen was then immersion fixed in 4% PFA. Specimens were imaged using a Nikon D850 DSLR camera with Nikon AF Micro-NIKKOR 200 mm f/4D IF-ED lens and scanned with a custom-built microCT at 50 kV and 200 μA with 260 μm resolution at the California Nanosystems Institute.

Neural Tracing Experiments

For initial surgery, following sedation (induction: ketamine 10 mg/kg IM/midazolam 1 mg/kg IM, maintenance: isoflurane 1-2% inhalation) and intubation, a right unilateral thoracotomy was performed by dividing the pectoral muscle, making a small incision in the pericardium, and exposing the right atrial (RA)-superior vena cava junction. Then 5 mg of an analog of 1,1'-dioctadecyl-3,3,3',3'-tetramethylindocarbocyanine perchlorate (*FAST* DiI, Invitrogen, D7756) in 250 μL of 100% methanol (MeOH) was injected using a 27-guage needle into the sinoatrial nodal (SAN) region. A chest tube was placed, and the incision was closed. Immediately prior to removal, the chest tube was aspirated. Tissues were harvested in a terminal procedure at least 3 weeks later as described below.

Porcine Tissue collection

Following sedation (induction: tiletamine-zolazepam 6 mg/Kg IM, maintenance: isoflurane 1-2% inhalation) and intubation, we performed a midline sternotomy and exposed the heart. A heparin bolus of 5000 U IV was administered, and the pig was then placed in ventricular fibrillation with application of a 9V battery to the surface of the heart. The heart was explanted and syringe-flushed with heparinized normal saline (5 U/mL) via the

transected aorta. The area of interest (RAGP-SAN region) was then excised and rinsed in heparinized saline. Whole-mount preparations of RAGPs for electron microscopy (EM) analysis were isolated under a dissection microscope and immersion fixed overnight at 4^{o}C in a 2% PFA and 2.5% glutaraldehyde solution in 0.12 mol/L Millonigs buffer (MB). RAGPs for histologic, tissue clearing and immunohistochemical studies were immersed in 4% PFA at 4^{o}C with agitation overnight. The following day, the tissues were washed three times for 30 minutes each in 0.01 mol/L PBS and stored in either 0.01 mol/L PBS and 0.02% sodium azide solution at 4^{o}C for histologic and tissue clearing studies or 0.01 mol/L PBS with 20% sucrose and 0.02% sodium azide for at least 1 week for cryopreservation for immunohistochemical studies. SAN region for RNA fluorescence in situ hybridization (RNAscope, ACD) was embedded in Optical Cutting Temperature compound (OCT, TissueTek) in a cryomold and placed on dry ice. Tissue was stored at -80^{o}C until processed. RAGPs for gene expression profiling were separated from the SANs, immersed in 0.01 mol/L PBS at room temperature (RT) for 30 seconds and transferred to 25% OCT, followed by 50% OCT and then embedded in 100% OCT and placed in a cryomold. The cryomold was placed in a MeOH dry ice bath for flash freezing.

Histologic Studies

Porcine and human epicardial RAGP fat pads and SANs were paraffin embedded and serially sectioned at 5 μm thickness. We obtained representative histologic sections and stained epicardial RAGP fat pad and SANs with hematoxylin and eosin (H&E) and Masson's trichrome using standard technique.[85] Slides were imaged on Aperio AT Turbo scanning machine at 20x.

iDISCO+ Tissue Clearing

Portions of porcine and pressure-perfused fixed human cardiac tissue were stained and cleared using the iDISCO+ protocol as previously described.[13, 18] Briefly, fixed tissue underwent graded MeOH dehydration (20, 40, 60 and 80% MeOH in diH_2O [vol/vol]) for 1 hour each at RT with agitation, washed twice with 100% MeOH for 1 hour at RT and incubated in 66% dichloromethane/33% MeOH overnight at RT with agitation. The following day, tissues were washed twice in 100% MeOH for 1 hour at RT, chilled at 4°C and then bleached in 5% H_2O_2 in MeOH (vol/vol) overnight at 4°C. Then, the tissues were rehydrated with a graded MeOH series and washed in 0.01 mol/L PBS for 1 hour each at RT with agitation. The tissues were washed in 0.01 mol/L PBS with 0.2% Triton X-100 for 1 hour at RT. Tissues were then stained by permeabilizing in 0.01 mol/L PBS, 0.2% Triton X-100, 20% dimethyl sulfoxide (DMSO) and 0.3 mol/L glycine and blocking in 0.01 mol/L PBS with 0.2% Triton X-100, 10% DMSO and 5% donkey serum, each for 2 days at 37°C with agitation. Tissues were then incubated in primary antibody rabbit anti-PGP9.5 (Abcam, ab108986, 1:200; **Online Table II**) diluted in 0.01 mol/L PBS with 0.2% Tween-20 and 10 mg/mL heparin (PTwH) for 1 week at 37°C with agitation. Tissues were washed 4 to 5 times in PTwH overnight at room temperature and incubated with secondary antibody donkey anti-rabbit Cy3 (Jackson ImmunoResearch, 711-165-152,1:300; **Online Table III**) for 1 week at 37°C with agitation. Primary and secondary antibodies were replenished midway through staining. Tissues were again washed in PTwH 4-5 times overnight at RT. To clear, tissues were dehydrated with a graded MeOH series as above and incubated in 66% dichloromethane/33% MeOH for 3 hours at RT with agitation.

Tissues washed twice in 100% dichloromethane for 15 minutes at RT and cleared, stored, and imaged in benzyl ether (Millipore Sigma, Catalog 108014; refractive index: 1.55).

Immunohistochemical Methods for Sections

Fixed specimens for porcine hearts containing the RAGP fat pad, SAN and RA were shipped to East Tennessee State University at 4°C in 0.01 mol/L PBS, 20% sucrose and 0.02% sodium azide solution. The fat pad and SAN with adjoining RA were dissected separately, frozen on dry ice, and stored at -80°C until sectioning. 30 μm thick sections were cut at -20 to -25°C using a Leica CM3050S cryostat (Leica Microsystems Inc.) and collected on charged slides. Tissues were sectioned in a plane parallel to the epicardial surface, and sections were collected in a sequence that yielded 8 sets of sections that each spanned the entire thickness of the specimen. Each set of tissue sections was stored at -20°C until further processing.

Slide-mounted tissue sections were immunostained at RT for markers using standard methods of fluorescence immunohistochemistry, as described previously.[21] Briefly, slides were rinsed with 0.01 mol/L PBS (pH 7.3), incubated for 10 minutes in 0.01 mol/L PBS containing 0.4% Triton X-100 and 0.5% bovine serum albumin (BSA), and blocked for 2 hours in 0.01 mol/L PBS containing 1% BSA, 0.4% Triton X-100, and 10% normal donkey serum (Jackson ImmunoResearch Laboratories). Each section was then incubated in blocking buffer containing one or more of the primary antibodies listed in **Online Table II**. Sections were washed again and incubated in blocking buffer before application of secondary antibodies. Species-specific donkey secondary antibodies conjugated to Alexa Fluor 488, 555, 594 or 647 (Jackson ImmunoResearch Laboratories)

were applied at a 1:200 dilution in 0.01 mol/L PBS containing 0.4% Triton X-100 and 1% BSA, and sections were incubated for 2 hours before final washing in 0.01 mol/L PBS (**Online Table III**). After final washes with 0.01 mol/L PBS, cover glasses were applied with Citifluor (Ted Pella, Inc.) or SlowFade Gold antifade reagent (Life Technologies Corporation). Specific staining did not occur in negative control sections processed without the addition of the primary antibodies.

Staining for tyrosine hydroxylase (TH) was amplified using a biotin-streptavidin method. Biotin-SP conjugated donkey anti-goat secondary antibody (Jackson ImmunoResearch Laboratories) was applied in place of regular secondary antibody and incubated for 2 hours. Sections were then washed with 0.01 mol/L PBS and incubated for 2 hours in streptavidin conjugated Cy3 (Jackson ImmunoResearch Laboratories).

Antibody Characterization

Specific primary and secondary antibodies used in this study are listed in **Online Tables II and III** along with the immunogen, host species, company, catalogue number, RRID number and dilution used. All primary antibodies were polyclonal except the mouse anti-CGRP (calcitonin gene-related peptide), which was monoclonal. Specificity of the antibodies was established based on the data provided by suppliers, published positive control staining, and positive and negative control staining conducted by us. Additional detail regarding primary antibodies has been previously described.[86] Specific staining was not detected when primary antibodies were omitted.

RNA Fluorescence In Situ Hybridization

The OCT-embedded SAN was equilibrated in the Leica cryostat at -20°C for 1 hour, and 20 µm sections were mounted on charged slides to undergo RNA fluorescence in situ hybridization (RNAscope, ACD) per the manufacturer's protocol. Briefly, sections were dried at -20°C for 2 hours and stored at -80°C until used. Slides were then immersed in chilled 4% PFA for 90 minutes at 4°C followed by 2 rinses with 0.01 mol/L PBS. Sections were dehydrated in a graded series of 50%, 70%, 100%, and 100% ethanol (EtOH in diH_2O; vol/vol) for 5 minutes each. The slides were then allowed to air dry for 5 minutes at RT and baked at 60°C for 30 minutes. A barrier around the section was created using a hydrophobic barrier pen and allowed to dry over 5 minutes. Slides were loaded in a humidity control tray, and 5 drops of H_2O_2 were added followed by a 10-minute incubation at RT. Slides were then washed with diH_2O twice. Five drops of Protease IV were added to each section and incubated for 30 minutes at RT in humidity control tray. Slides were then washed with 0.01 mol/L PBS twice. Five drops of each probe mix were added to each slide. Probe mixes included a negative control, positive control mix (*PPIB*, *POLR2A-C2* and *UBC-C3*) and *HCN4*. Slides were baked at 40°C for 2 hours in a humidity control tray. In this and the subsequent washing steps, slides were washed with wash buffer for 2 minutes twice. Five drops of Multiplex FL v2 Amp 1 were added to each slide and baked at 40°C for 30 minutes. After washing, 5 drops of Multiplex FL v2 Amp 2 were added to slides, and the slides were baked at 40°C for 30 minutes. Slides were and 5 drops of Multiplex FL v2 Amp 3 were added to each slide and baked for 15 minutes at 40°C. Slides were washed and then 5 drops of Multiplex FL v2 HRP-C1 were added to each slide and baked for 15 minutes at 40°C. After washing, 150 µL of Opal 690 dye (1:1500 in DMSO) was added to each slide and incubated for 30 minutes at 40°C. Following another wash,

5 drops of Multiplex FL v2 HRP blocker were added, and slides baked at 40°C for 15 minutes. After washing, 5 drops of Multiplex FL v2 HRP-C2 were added to each slide and baked at 40°C for 15 minutes. After another wash, 150 µL of Opal 570 dye to each slide and incubated for 30 minutes at 40°C. After washing, 5 drops of Multiplex FL v2 HRP blocker were added to each slide and incubated at 40°C for 15 minutes. Following washing, 4 drops of DAPI was added to each slide, incubated for 30 seconds at RT, and then tapped dry. One drop of ProLong Gold Antifade Mountant was added to each slide and coverslipped. Slides were left to dry overnight in the dark and stored at 4°C until imaging.

Immunohistochemical Method for Ganglion Whole-Mount Preparations

After electrophysiologic recordings (see below), isolated ganglia were fixed in 4% PFA overnight. Fixed tissue was washed in 0.01 mol/L PBS 3 times for 1 hour each and stored in 0.01 mol/L PBS with 0.02% sodium azide. The tissue was blocked in 0.01 mol/L PBS, 0.02% sodium azide, 0.2% Triton X-100 and horse serum for 4 hours at RT with agitation. The following primary antibodies were used: rabbit anti-PGP9.5 (1:500), sheep anti-TH (1:200) in 0.01 mol/L PBS, 0.02% sodium azide and 0.2% Triton X-100 with agitation for 2 nights (**Online Table II**). Tissues were washed with a solution of 0.01 mol/L PBS with 0.02% sodium azide every hour for 3 hours. Tissue was incubated in secondary antibodies diluted in 0.01 mol/L PBS with 0.1% Triton X-100 and 0.02% sodium azide for 2 nights at RT with agitation. The following secondary antibodies were used: donkey anti-rabbit Cy3 (1:200), donkey anti-sheep 488 (Jackson ImmunoResearch, 713-545-147, 1:200; **Online Table III**). Secondary staining with streptavidin conjugated ATTO-647N

was used to visualize neurobiotin filling (1:500). Stained tissue was rinsed in 0.01 mol/L PBS with 0.02% sodium azide every hour for 3 hours, mounted on glass slides, and coverslipped.

Imaging and Image Processing

Slides were viewed under fluorescence illumination with an Olympus BX41 microscope equipped with an Olympus DP74 digital camera and cellSens software (Olympus America Inc., Center Valley, PA, RRID:SCR_016238). For quantitative studies of the RAGP, SAN and adjoining RA, slides were evaluated with a Leica TCS SP8 Confocal Microscope with 10x, 20x and 40x objective lenses (Leica Microsystems Inc.). Confocal images were collected at a resolution of 1024 x 1024 using 488, 552 and 638 nm laser lines. Stacks spanned tissue thicknesses of 25-33 μm unless otherwise noted. Figures were created using maximum intensity projection (MIP) images for individual channels and merged images. For quantitative studies of the neurochemical phenotype of neurons in the RAGP, confocal images were collected for every ganglion (≥ 3 neurons) in one set of section for each pig. For quantitative studies of nerve fiber density in the SAN and RA, ten 30x confocal images from separate fields, usually on different sections and slides, were collected for each pig.

Each iDISCO+-cleared tissue was placed in a chamber (SunJin Lab) filled with benzyl ether on a slide, and a coverslip applied. Tilescan and Z stack images were obtained using a Zeiss LSM 880 confocal laser scanning microscope with a Fluar 5x/0.25 M27 Plan-Apochromat and 10x lens. Images were obtained at a resolution of 1024 x 1024 using 488 and 561 nm laser lines. Z-axis step size was commensurate with Nyquist

sampling based on numerical aperture of the specified objective. Pinhole was set to 1 airy unit. Stitched images were analyzed in Zeiss Zen Black SR and Bitplane Imaris 9.5.1 for 3-dimensional visualization.

In situ hybridization sections and RAGP whole-mount preparations (protocol described in Supplementary Material) were imaged with an upright laser scanning confocal microscope (Zeiss AxioExaminer/LSM 880). For the RNA fluorescence in situ hybridization studies, 8-bit tile scan images were obtained using a Plan-apochromat 20x/0.8 objective lens. For the whole-mount preparations, tilescan and Z-stack images (8-bit) were acquired using both low-power (W Plan-Apochromat 10x/0.5 M27 75 mm) and high-power (Plan-Apochromat 63x/1.40 Oil DIC M27) objectives to scan whole tissue (cm^2) or individual ganglia (μm^2), respectively. Z-axis step size and pinhole were set as mentioned above. Laser excitation of fluorophores (DAPI: 405 nm diode laser; Opal 570 and Cy3: 561 nm diode pumped solid state laser; Alexa Fluor 488: 488 nm argon laser; Opal 690 and ATTO 647: 633 nm HeNe laser) was optimized for maximum gain without oversaturation of the detector. Muscle autofluorescence was obtained using the 488 nm laser line. Stitched images were analyzed in Zeiss Zen Black SR.

Image Analysis

The RAGP fat pads from pigs injected with DiI into the SAN region were sectioned as described above. Sections were first evaluated without attaching cover glasses, and images of every ganglion were collected using the Olympus fluorescence microscope and camera. This approach was taken because some DiI would be lost during subsequent immunohistochemical staining. After documenting DiI labeled neurons, the sections were

immunolabeled for PGP9.5 to identify all neurons in the ganglia. For each ganglion, we were then able to count DiI-labeled neurons and the total number of neurons (i.e., PGP9.5-positive).

Quantification of RAGP neurons singly or doubly labeled for specific neuronal markers was done using Stereo Investigator software v2019.1.1 (MicroBrightField, Inc., RRID:SCR_002526). Unique markers were used to differentiate total neuron count, single and double labeled neurons.

Nerve density in cardiac regions was determined by using ImageJ software to evaluate single channel confocal images that were labeled for VAChT (vesicular acetylcholine transporter), TH (tyrosine hydroxylase) and NPY (neuropeptide Y). Nerve density was calculated as the area occupied by nerves as a percentage of the entire image area and reported as % area.

Colocalization of two markers in nerve fibers was evaluated using maximum intensity projection (MIP) confocal images. The colocalization rate was quantified in select images using a module of the Leica LASX Software (RRID:SCR_013673). This module displays a two-channel image as a scatter plot that is used to adjust thresholds so that only points of pixel overlap are retained, and the background is removed. Colocalization rate is reported as a percentage of colocalization area/total area.

Transmission Electron Microscopy

After MB and double-distilled H_2O (ddH_2O) washes, the tissues were fixed in 1% osmium solution diluted in ddH_2O followed by dehydration in ethanol (EtOH) and propylene oxide. The tissues were blocked and embedded in Epon plastic resin (Ted Pella). Semi-thin

cross sections (0.5 μm) were obtained and labeled with 1% toluidine blue solution diluted in ddH_2O for overview visualization of RAGP organization at light microscopy level using a Nikon Eclipse E600 microscope and Nikon camera DS-Fi3. Ultrathin sections (70nm thickness) were collected on formvar coated grids (Ted Pella), counterstained with uranyl acetate and lead citrate, and examined under a Tecnai G2 Spirit Twin transmission electron microscope (FEI, ThermoFisher Scientific) operating at 80 kV and images acquired with a Gatan Orius SC 1000B digital camera (Gatan) for detailed characterization of the RAGP organization.

Cryosectioning and Staining for Laser Capture Microdissection and High-Throughput Real-Time Quantitative Reverse Transcription Polymerase Chain Reaction (qRT-PCR)

RAGP was consecutively sectioned at 40 μm thickness along the superior-inferior vena caval axis, imaged and mounted on PPS membrane slides (Leica Microsystems, Catalog 11600294). An average of 400 slides were generated per RAGP. Slides were fixed in ice-cold 100% EtOH for 1 minute followed by 4 minutes of staining with 0.0001% Cresyl Violet (ACROS Organics, AC229630050). Slides were dehydrated using 95% and 100% EtOH followed by xylene for 1 minute each. RNAse inhibitor (Invitrogen SUPERase-In RNase Inhibitor, Catalog AM2696) was added to all aqueous reagents to preserve RNA quality.

Laser Capture Microdissection

Samples were collected immediately post-staining using laser capture microdissection (LCM; Arcturus, ThermoFisher). Single neurons were visualized in the 0.0001% cresyl-violet stained sections using a brightfield and triple filter. Samples were collected on LCM caps and stored at -80^{o}C. Samples were lysed at the time of high-throughput real-time qRT-PCR experiments with lysis reagents as described below.

Mapping LCM samples onto the reconstructed 3-dimensional stack

2-dimensional blockface images generated for each tissue section during cryosectioning were used to generate a 3-dimensional volume in Tissue Mapper software (MicroBrightField, Inc.). Images taken during LCM sample collection were referenced to corresponding sections in the 3-dimensional stack. Anatomical features and neurons were assigned markers enabling extraction of specific XYZ coordinates.

High-throughput Real-Time qRT-PCR

Single RAGP neurons in lysis buffer (Cells Direct Lysis Buffer, Invitrogen) were processed for reverse transcription using SuperScript VILO Master Mix (Thermo Fisher Scientific) followed by RT-PCR for targeted amplification and detection using the Evagreen intercalated dye-based approach to detect the PCR-amplified product. Intron-spanning PCR primers were designed for every assay using Primer3[87] and BLAST.[88] Genes selected spanned a variety of neuronal functions, signal transduction and cell-type identification. Per the standard BioMark protocol, cDNA samples were processed for 22 cycles of specific target amplification of 283 genes using TaqMan PreAmp Master Mix as

per the manufacturer's protocol (Applied Biosystems). Real-time PCR reactions were performed using 96.96 BioMark Dynamic Arrays (Fluidigm) enabling quantitative measurement of multiple mRNAs and samples under identical reaction conditions. Each run consisted of 30 amplification cycles (15 seconds at 95°C, 5 seconds at 70°C, 60 seconds at 60°C). Real-Time PCR Analysis Software (Fluidigm) was used to calculate Ct values. Twenty-one 96 × 96 BioMark Arrays were used to measure gene expression across the 422 (before QC) single-cell samples. The same serial dilution sample set was included in each chip to assess batch effects. Samples from each RAGP were run across 3 chips to obtain data on 283 genes per sample. Each set of chip runs for a given animal contained overlapping assays that served as technical replicates to evaluate chip-to-chip variability, which was minimal.

High-throughput qRT-PCR data analysis

Melt-curve analysis was used to assess quality of qRT-PCR results. Samples with >30% failed reactions and genes with >20% failed reactions were excluded from analysis. An additional 10 samples were outliers and excluded from analysis. A total of 405 single-cell samples and 246 different gene assays were included in the final analysis. Raw Ct values for individual samples were normalized against a median expression level of a subset of 140 robustly expressed genes (genes with greater than 60% working reactions) across all animals to obtain $-\Delta Ct$ values. The vector of median sample expression value was chosen over potential reference genes based on comparison of stable expression across all samples against known housekeeping genes using the 'selectHKs' function in the

NormqPCR package in R. The -ΔCt data were then rescaled using the median across all samples within a gene using the following equation:

$$-\Delta\Delta Ct_{gene} = -\left(\Delta Ct_{sample} - \Delta Ct_{across\text{-}sample\text{-}median}\right)$$

The raw and normalized dataset is available online as a Gene Expression Omnibus dataset (GEO reference ID: GSE149212). Pearson correlation was performed to compare gene expression levels and generate heatmaps.

Intracellular Recordings from Intrinsic Cardiac Neurons

Tissue was isolated as above and placed in ice-cold physiologic salt solution (PSS) containing in mM: 121 NaCl, 5.9 KCl, 1.2 NaH_2PO_4, 1.2 $MgCl_2$, 25 $NaHCO_3$, 2 $CaCl_2$, 8 D-glucose; pH 7.4 maintained by 95% O_2/5% CO_2 aeration. Ganglia of the RAGP were isolated from the surface of the inferior vena cava-RA junction in proximity (~5-10 mm) to the SAN. Isolated whole ganglia were pinned to the SylGard (Dow Corning) floor of a glass bottom petri dish. RAGP neurons were observed with an upright microscope (Zeiss AxioExaminer) equipped with a 5x and a 40x water-immersion objective.

Intracellular measurements of membrane potential were obtained following technique described previously.[89] Preparations of ganglia were continuously superfused (6–7 mL/min) with PSS maintained at 32–35°C with a thermostatically controlled heater. Neurons were impaled with borosilicate-glass microelectrodes filled with 2 mol/L KCl + 2% Neurobiotin (80-160 MΩ; Vector Labs). Membrane voltage was recorded with a Multiclamp 700B amplifier connected to a Digidata 1550B data acquisition system. pCLAMP 10 software (Molecular Devices) was used for data acquisition and analysis. Depolarizing and hyperpolarizing currents were applied through the recording electrode

to characterize neuronal membrane properties. Hyperpolarizing steps (-100 pA, 500 ms) were given to measure steady state input resistance. Depolarizing current steps (0.1–0.5 nA, Δ 100 pA, 500 ms duration) were used to assess neuronal excitability. Inclusion criteria for analysis included a resting membrane potential less than -40 mV, a holding current of greater than -100 pA, and cells must generate an action potential.

Concentric bipolar stimulation electrodes (FHC) were placed onto interganglionic nerves. Graded stimulus shocks (100 μs) in 50-100 μA steps, from 0 to 800 μA were used to generate stimulus recruitment curves (Master 8 and IsoFlex optical Isolation unit, AMPI). Five to 20 stimuli were delivered at each stimulus intensity, with an interval of 3 seconds between stimuli. At least two stimulating electrodes were used to activate discrete nerve bundles into a single ganglion. After electrophysiologic recordings, isolated ganglia were fixed in 4% PFA overnight and prepared for immunostaining as described above.

Ablation of Porcine RAGP

Surgery was performed as above except a clamshell thoracotomy was performed for improved exposure of the RAGP. Following thoracotomy, anesthesia was changed to α-chloralose (50 mg/Kg intravenous bolus administration followed by continuous infusion at 10 mg/Kg/hr IV). The left and right cervical vagi were dissected free in the neck and encircled with platinum nerve cuff electrodes. A quadripolar His catheter (Abbott) was placed via the right external jugular vein and advanced until a His signal was visualized while a quadripolar catheter was inserted via the right femoral vein and advanced to the RA. The left and right stellate ganglia were dissected free and either platinum needle

electrodes or cuff electrodes were placed. All stimulations were performed individually using a Grass S88 Stimulator via PSIU6 constant current isolation units. Square wave stimulation pulses (10 Hz frequency, 1 ms duration, 0.1-15 mA) were delivered individually to each vagus nerve, and stimulus threshold was defined as the stimulation current strength that was sufficient to elicit a 10% decrease in heart rate. Current amplitude was increased to 3 times threshold for all subsequent vagal nerve stimulation (VNS). Square wave stimulation pulses (4 ms duration, 4 Hz frequency, 0.1-15 mA) were delivered individually to each ganglion or sympathetic chain. Stimulus threshold was defined as the stimulation current strength that was sufficient to elicit a 10% increase of left ventricular end-systolic pressure (LVESP) or heart rate. Current amplitude was increased to 3 times threshold for all subsequent sympathetic stimulations. Right atrial pacing was performed using a Micropace EPS320 system at 2 times capture threshold at a rate at least 20% greater than the resting heart rate during the last 10 seconds of each VNS.

Continuous 12-lead surface ECG and intracardiac ECG data were recorded using a Prucka CardioLab (GE Healthcare). For ARI recordings, a custom 56-electrode sock, placed over both ventricles, was connected to the Prucka CardioLab system to identify regional activation recovery intervals (ARI). Global ventricular ARIs were calculated via customized software ScalDyn M (University of Utah), as described previously.[90] ARI, a surrogate marker of local action potential duration, was calculated as the difference between the first minimal dV/dt in the QRS complex to the first maximal dV/dt of the T wave.

Systolic left ventricular (LV) pressures were assessed by using a 5 Fr pigtail, 12-pole conductance-pressure catheter connected to an PCU-2000 Pressure Control Unit (Millar Instruments, Inc.) placed in the LV via carotid or femoral artery sheath under ultrasound guidance. Pressure was continuously monitored and recorded throughout experiments. Systolic LV function was assessed by LV end-systolic pressure (LVESP) and the maximum rate of LV pressure change (dP/dt_{max}). Data were acquired using the Cambridge Electronic Design System and Spike2 software. Heart rates and atrial-His (AH) intervals were measured in Spike2 software.

After baseline stimulations at 3 times threshold of the bilateral stellate ganglia and cervical vagi were performed, the RAGP was ablated using a Stryker Sonopet ultrasonic aspirator. After the RAGP was ablated, repeat VNS with atrial pacing and SGS were performed.

Electrical Recordings of SAN Region

After thoracotomy, instrumentation of bilateral vagi and stellate ganglia and placement of RA and His catheters as above, a custom-made 64-channel multielectrode array (Neuronexus) was positioned over the sulcus terminalis and electrical recordings were acquired using an Alpha Omega system. The bilateral vagi and stellate ganglia were individual stimulated at 3 times threshold as above and recordings at the SAN performed. Then, platinum needle electrodes were inserted to the RAGP and stimulated using the Grass S88 Stimulator via PSIU6 constant current isolation units. Square wave stimulation pulses (50 Hz frequency, 0.1 ms duration, 0.1-15 mA) were delivered until a heart rate decrease of at least 10% was noted. Analysis of SAN recordings was performed using

customized ScalDyn M software. Activation times (Ats) were measured from the beginning of the P wave to the first minimal dV/dt in the atrial electrogram.

Right Atrial Wedge Preparation and Optical Mapping

For optical mapping of the human SAN, the entire RA was carefully isolated, and the right coronary artery was cannulated with a custom flexible plastic cannula. Bleeding vessels were tied off, and the tissue was stretched across a custom frame and transferred to a vertical bath of warmed (37°C) and oxygenated (95% O_2/5% CO_2) Tyrode's solution (in mM: 128.2 NaCl, 4.7 KCl, 1.05 $MgCl_2$, 1.3 $CaCl_2$, 1.19 NaH_2PO_4, 20 $NaHCO_3$, 11.1 Glucose). Adequate perfusion was maintained for the duration of the experiment for tissue viability, and sensing electrodes were pinned into the bath for pseudo-ECG recordings using LabChart. The preparation was electromechanically uncoupled with blebbistatin (10-15 μM) and fluorescently stained with di-4-ANEPPS. Optical action potentials (OAPs) were captured with MiCAM05 CMOS cameras with high spatial and temporal resolutions (100 × 100 pixels, 1 kHz sampling frequency; SciMedia). During recordings, the endocardial surface of the tissue was illuminated with a 520 nm LED (Prizmatix), and emitted fluorescence was captured through a 650 nm long-pass filter (Thorlabs).

RHYTHM, a custom-made MATLAB program designed for optical mapping data analysis, was used for the creation of optical activation maps and identification of the leading pacemaker sites. OAPs were spatially (5 x 5 pixel neighborhood) and temporally (low pass Butterworth filter at 150–200 Hz) filtered, and 60 Hz noise was removed. Baseline fluorescent drift was also removed with a first- or second-order fitted curve, and activation maps were created by identifying 50% of the maximum OAP amplitude.

Stimulation of the RAGP was performed with a bipolar stimulus electrode placed on the epicardial fat pad at frequencies of 50 Hz and 100 Hz with a pulse width of 200 μs.

Statistics

GraphPad Prism 8.4.2 was used for data analysis and graph generation. Based on preliminary GP ablation experiments, we estimated we would need 4 pigs to detect a 40% bradycardia with a standard deviation of 20% at an α level of 0.05 at 80% power in paired difference analysis for the functional experiments. Sample sizes are included in figure legends or text and in **Online Table IV**. Normality of data was assessed using the Shapiro-Wilk test, and data are presented as mean ± SD for normally distributed data or as median (interquartile range [IQR]) for non-normally distributed data. Analysis of ventricular ARI with VNS and pacing was performed using repeated measures ANOVA. Comparisons of heart rate and left ventricular contractility pre- and post-RAGP ablation or stimulation were conducted using a two-tailed paired Student's t-test for normally distributed data or Wilcoxon matched-pairs signed rank test for non-normally distributed data. $P < 0.05$ was considered statistically significant. Correction for multiple hypothesis testing was performed within, but not across, tests.

Data Availability

Raw and processed high-throughput real-time qRT-PCR data of single neurons from the pig RAGP have been deposited in the GEO database under accession code: GSE149212. All sample acquisition images, raw and processed transcriptomic data, and annotations pertaining to 3-dimensional spatial location are publicly available in the

sparc.science repository with the identifiers 10.26275/56h4-ypua, 10.26275/5jki-b4er and 10.26275/qkzi-b1mq.

Online Table I. Clinical information for human cardiac specimens

Source	Age	Sex	Clinical Information	Experiment
Cadaver	97	F	History of coronary artery disease who died of cardiopulmonary failure	Contrast injection into coronary artery
Donor heart	31	M	No cardiac history, died of anoxia (hanging)	Histology
Donor heart	71	F	History of diabetes mellitus and hypertension who died following a large intracranial hemorrhagic stroke	Tissue clearing
Donor heart	52	F	History of hypertension and hyperlipidemia who died of stroke	Optical mapping

Online Table II. Primary Antibodies

Antibody	Host	Immunogen	Company	Catalog No.	RRID	Dilution
Anti-VAChT (vesicular acetylcholine transporter)	Rabbit	aa 475-530 from rat VAChT	Synaptic Systems	139 103	AB_887864	1:500
Anti-TH (tyrosine hydroxylase)	Sheep	Native TH from rat pheocromocytoma	Millipore	AB1542	AB_90755	1:500; 1:200 (whole-mount)
	Rabbit	SDS-denatured rat tyrosine hydroxylase, purified from pheochromocytoma	Pel-Freez Biologicals	P40101-150	AB_2313713	1:1000
Anti-VMAT2 (vesicular monoamine transporter 2)	Rabbit	Synthetic peptide (aa 1-20 from mouse VMAT2)	Synaptic Systems	138313	AB_2619826	1:200
Anti-NPY (neuropeptide Y)	Rabbit	Synthetic NPY coupled to bovine thyroglobulin (BTg)	ImmunoStar	22940	AB_2307354	1:1000
Anti-MAP2 (microtubule-associated protein 2)	Chicken	Recombinant fragment of human MAP2, aa 235-1588	Abcam	ab5392	AB_2138153	1:1000
Anti-SP (substance P)	Rabbit	Synthetic SP coupled to KLH	ImmunoStar	20064	AB_572266	1:1000
Anti-VIP (vasoactive intestinal peptide)	Rabbit	Porcine VIP coupled to BTg	ImmunoStar	20077	AB_2572270	1:1000
Anti-Somatostatin	Rabbit	Synthetic SOM coupled KLH	ImmunoStar	20067	AB_572264	1:1000
Anti-nNOS (neuronal nitric oxide synthase)	Goat	aa 1423-1434 of human NOS1	Abcam	ab1376	AB_300614	1:1000
Anti-PGP9.5 (protein gene product 9.5)	Rabbit	Synthetic peptide to residues in Human PGP9.5	Abcam	ab108986	AB_10891773	1:500; 1:200 (iDISCO+)
Anti-S100	Rabbit	S100 isolated from cow brain	Dako	GA504	AB_2811056	1:400
Anti-ChAT (choline acetyltransfer-ase)	Goat	Human placental enzyme	Millipore	AB144P	AB_2079751	1:25
Anti-CGRP (calcitonin gene-related peptide)	Goat	Rat CGRP C-terminal peptide, VKDNFVPTNVGS EAF	Abcam	ab36001	AB_725807	1:1000
	Mouse	Rat alpha-CGRP	Abcam	ab81887	AB_1658411	1:1000
Anti-Connexin 43	Rabbit	Synthetic peptide conjugated to KLH with glutaraldehyde	Sigma-Aldrich	C6219	AB_10745285	1:800

Online Table III. Secondary Antibodies

Antibody	Host	Company	Catalog No.	RRID	Dilution
Cy3-conjugated Streptavidin	-	Jackson ImmunoResearch Laboratories, Inc.	016-160-084	AB_2337244	1:900
Atto 647N-Streptavidin	-	Sigma-Aldrich	94149	-	1:500
Biotin-SP-conjugated AffiniPure Donkey Anti-Goat IgG	Donkey	Jackson ImmunoResearch Laboratories, Inc.	705-065-147	AB_2340397	1:200
Alexa Fluor 488-conjugated AffiniPure Donkey Anti-Sheep IgG	Donkey	Jackson ImmunoResearch Laboratories, Inc	713-545-147	AB_2340745	1:200
Cy3 AffiniPure Donkey Anti-Rabbit IgG	Donkey	Jackson ImmunoResearch Laboratories, Inc	711-165-152	AB_2307443	1:300
Alexa Fluor 594-conjugated AffiniPure Donkey Anti-Goat IgG	Donkey	Jackson ImmunoResearch Laboratories, Inc.	705-585-147	AB_2340433	1:200
Alexa Fluor 594-conjugated AffiniPure Donkey Anti-Mouse IgG	Donkey	Jackson ImmunoResearch Laboratories, Inc.	715-585-150	AB_2340854	1:200
Alexa Fluor 488-conjugated AffiniPure Donkey Anti-Rabbit IgG	Donkey	Jackson ImmunoResearch Laboratories, Inc	711-545-152	AB_2313584	1:200
Alexa Fluor 594-conjugated AffiniPure Donkey Anti-Rabbit IgG	Donkey	Jackson ImmunoResearch Laboratories, Inc	711-585-152	AB_2340621	1:200
Alexa Fluor 594-conjugated AffiniPure Donkey Anti-Chicken IgG	Donkey	Jackson ImmunoResearch Laboratories, Inc.	703-585-155	AB_2340377	1:200
Alexa Fluor 647-conjugated AffiniPure Donkey Anti-Chicken IgG	Donkey	Jackson ImmunoResearch Laboratories, Inc.	703-605-155	AB_2340379	1:200
Alexa Fluor 647-conjugated AffiniPure Donkey Anti-Rabbit IgG	Donkey	Jackson ImmunoResearch Laboratories, Inc	711-605-152	AB_2492288	1:200
Cy3 AffiniPure Donkey Anti-Rabbit IgG	Donkey	Jackson ImmunoResearch Laboratories, Inc	711-165-152	AB_2307443	1:300

Online Table IV. List of comparisons across immunohistochemical and RAGP ablation and stimulation experiments

								p-value	
Figure	Comparison (s)	Normality test	p- value	Passed normality test (alpha = 0.05)?	Sample size	Statistical test	Correction for multiple hypothesis testing	Unadjusted	Adjusted
4E	VAChT SAN vs TH SAN	Shapiro-Wilk	0.9	Yes	4	Kruskal-Wallis	Dunn's	-	0.085
4E	VAChT SAN vs VAChT Atrium	Shapiro-Wilk	0.9	Yes	4	Kruskal-Wallis	Dunn's	-	0.006
4E	TH SAN vs TH Atrium	Shapiro-Wilk	0.9	Yes	4	Kruskal-Wallis	Dunn's	-	>0.99
4E	VAChT Atrium vs TH Atrium	Shapiro-Wilk	0.9	Yes	4	Kruskal-Wallis	Dunn's	-	0.48
4H	NPY SAN vs TH SAN; NPY SAN vs NPY Atrium; NPY Atrium vs TH atrium; TH SAN vs TH Atrium	Shapiro-Wilk	0.23	Yes	4	Kruskal-Wallis	Dunn's	0.49	-
4I	VAChT/TH SAN vs NPY/TH SAN	Shapiro-Wilk	0.13	Yes	4	Kruskal-Wallis	Dunn's	-	0.03
4I	VAChT/TH SAN vs VAChT/TH Atrium	Shapiro-Wilk	0.13	Yes	4	Kruskal-Wallis	Dunn's	-	>0.99
4I	NPY/TH SAN vs NPY/TH Atrium	Shapiro-Wilk	0.13	Yes	4	Kruskal-Wallis	Dunn's	-	>0.99
4I	VAChT/TH Atrium vs NPY/TH Atrium	Shapiro-Wilk	0.13	Yes	4	Kruskal-Wallis	Dunn's	-	0.15
7C	Baseline HR vs RAGPx HR	Shapiro-Wilk	0.42	Yes	7	Paired t-test	-	0.031	-
7D	RCVNS Baseline vs RCVNS RAGPx	Shapiro-Wilk	0.64	Yes	7	Paired t-test	-	0.0002	-
7D	LCVNS Baseline vs LCVNS RAGPx	Shapiro-Wilk	0.14	Yes	7	Paired t-test	-	0.0010	-
7D	RSGS Baseline vs RSGS RAGPx	Shapiro-Wilk	0.14	Yes	7	Paired t-test	-	0.066	-
7D	LSGS Baseline vs LSGS RAGPx	Shapiro-Wilk	0.47	Yes	7	Paired t-test	-	0.53	-
7D	RCVNS Baseline LV dP/dt_{max} vs RCVNS RAGPx LV dP/dt_{max}	Shapiro-Wilk	0.57	Yes	7	Paired t-test	-	0.0004	-
7D	LCVNS Baseline LV dP/dt_{max} vs LCVNS RAGPx LV dP/dt_{max}	Shapiro-Wilk	0.11	Yes	7	Paired t-test	-	0.014	-
7D	RSGS Baseline LV dP/dt_{max} vs RSGS RAGPx LV dP/dt_{max}	Shapiro-Wilk	0.048	No	7	Wilcoxon matched-pairs signed rank	-	0.11	-
7D	LSGS Baseline LV dP/dt_{max} vs LSGS RAGPx LV dP/dt_{max}	Shapiro-Wilk	0.80	Yes	7	Paired t-test	-	0.61	-
7E	RCVNS Baseline AH vs RCVNS RAGPx AH	Shapiro-Wilk	0.41	Yes	6	Paired t-test	-	0.015	-
7E	LCVNS Baseline AH vs LCVNS RAGPx AH	Shapiro-Wilk	0.43	Yes	5	Wilcoxon matched-pairs signed rank	-	0.13	-
8C	Baseline HR vs RAGP Stim HR	Shapiro-Wilk	0.0016	No	8	Wilcoxon matched-pairs signed rank	-	0.008	
Online Figure X	RCVNS Baseline Prestim ARI vs RCVNS Baseline Stim and Pacing vs RCVNS RAGPx Prestim vs RCVNS RAGPx Stim and Pacing	-	-	-	7	Repeated measures ANOVA	Sidak's multiple comparisons test	ns	-

Online Figure X	LCVNS Baseline Prestim ARI vs LCVNS Baseline Stim and Pacing vs LCVNS RAGPx Prestim vs LCVNS RAGPx Stim and Pacing	-	-	-	7	Repeated measures ANOVA	Sidak's multiple comparisons test	ns	-

Abbreviations: AH indicates atrial-His interval; ARI, activation-recovery interval; dP/dt_{max} maximum rate of LV pressure change HR, heart rate; LCVNS, left cervical vagal nerve stimulation; LSGS, left stellate ganglion stimulation; NPY, neuropeptide Y; pacing, atrial pacing; prestim, prior to vagal nerve stimulation; RAGP, right atrial ganglionated plexus; RAGPx, RAGP ablation; RCVNS, right cervical vagal nerve stimulation; RSGS, right stellate ganglion stimulation; SAN, sinoatrial node; stim, vagal nerve stimulation; TH, tyrosine hydroxylase; VAChT, vesicular acetylcholine transporter.

Online Table V. Primers for neuron-specific genes used in high-throughput real-time qRT-PCR experiments

Gene	Forward Primer	Reverse Primer
NEUN	GTTTACCTCCCAACCCGAGG	CTCGGCTGTGCCACTTTTTC
PGP9.5	TGCCTTTTCCGGTGAACCAT	AACGGGGATAAAGCGAAGGG
MAP2	TGCCGGGGAAGGTGTACTTA	TCTTCTTCTGCGCCTTGCAT

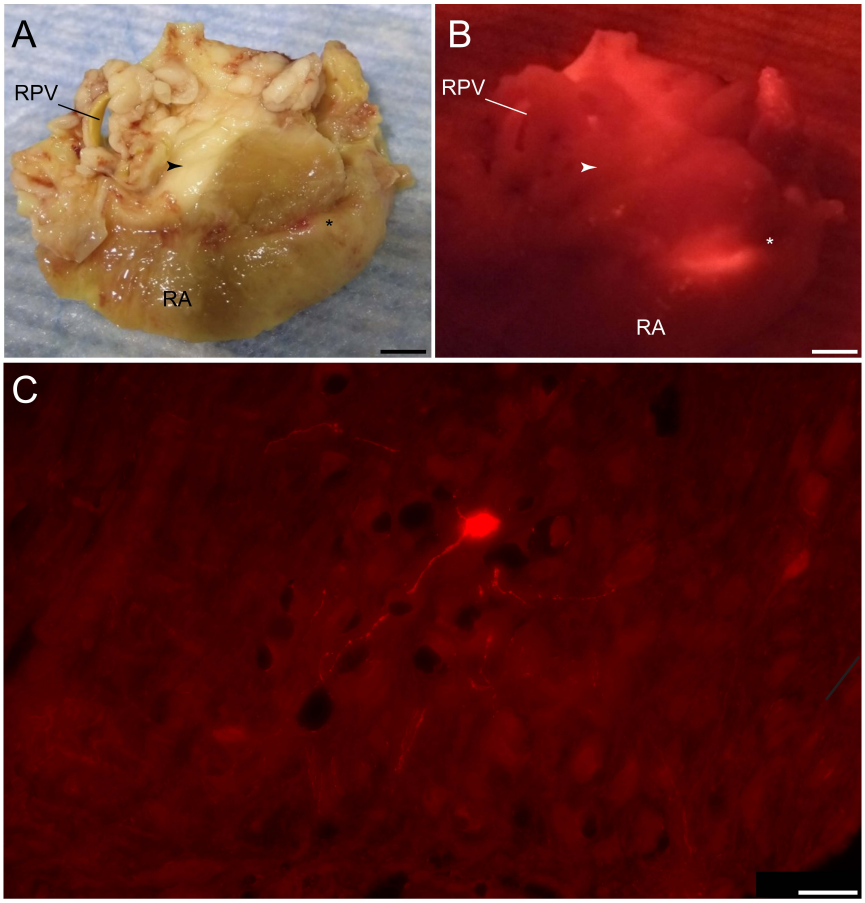

Online Figure I. Injection site of DiI retrograde tracer in the sinoatrial nodal (SAN) region. A, Brightfield photomicrograph of anterior view of heart showing right atrial ganglionated plexus (RAGP; arrowhead) and SAN (*) region. **B**, Fluorescence photograph of the same regions (RAGP: arrowhead; SAN: *) showing the DiI injection site. RA indicates right atrium; RPV, right pulmonary vein. **C**, Confocal image of a neuron in right stellate ganglion labeled with DiI. Scale bar are 5 mm (**A**, **B**) and 200 μm (**C**).

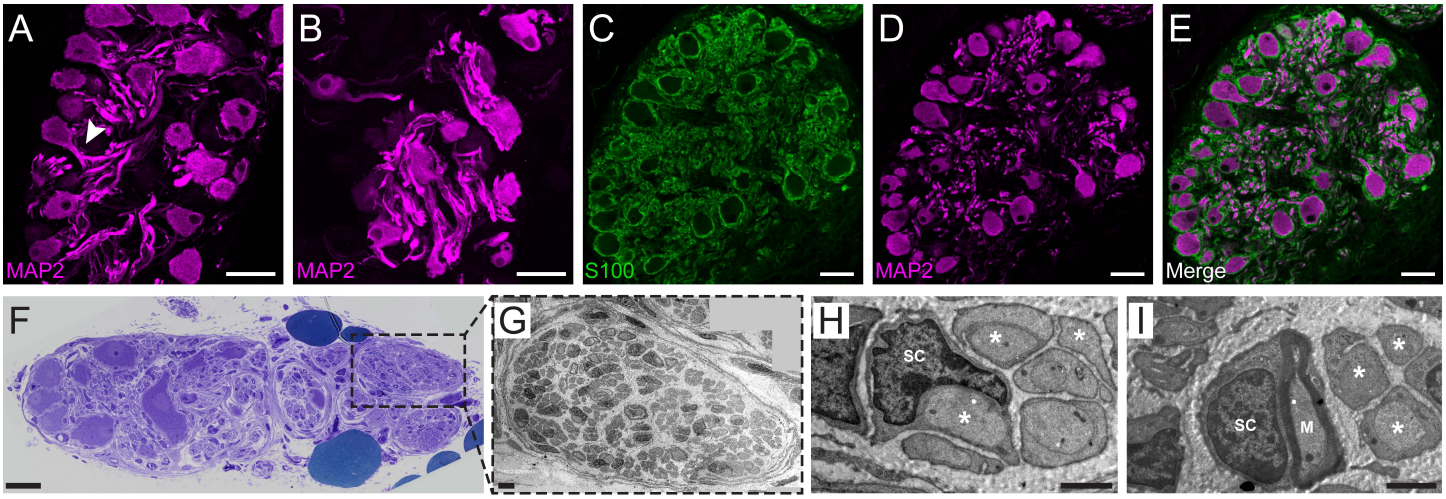

Online Figure II. Immunohistochemical and electron microscopic phenotyping of ganglia in the porcine right atrial ganglionated plexus (RAGP) fat pad. A-B, Ganglia stained for MAP2 (mitrotubule-associated protein 2) contain many multipolar neurons, some with one or more thick processes and a variable number of thinner processes. Some of the latter appear short, likely due the plane of sectioning and others are longer. Occasionally, axons bifurcate after leaving the cell body (**A**, arrowhead). **C-E**, Neurons in the porcine RAGP are surrounded by satellite glial cells. Ganglia were double labeled for the glial marker S100 and the pan-neuronal marker MAP2 (**C-D**), and corresponding overlay images (**E**) show that S100-positive cells and processes surround MAP2-positive perikarya, axons and other processes. **F**, Light microscopy image of toluidine blue staining of RAGP shows several distinct sub-compartments, some with ganglionic neurons and some without neurons. **G-I**, Ultrastructural detail of RAGP fascicle with numerous unmyelinated fibers (*) and some myelinated fibers. Note Schwann cell nuclei in P (SC) and one to one close relationship between myelinated axon (M) and Schwann cell in **I**. 4 (2 male, 2 female) porcine RAGPs were evaluated in the electron microscopy studies. Scale bars are 50 μm (**A-E**), 30 μm (**F**), and 0.5 μm (**G-I**).

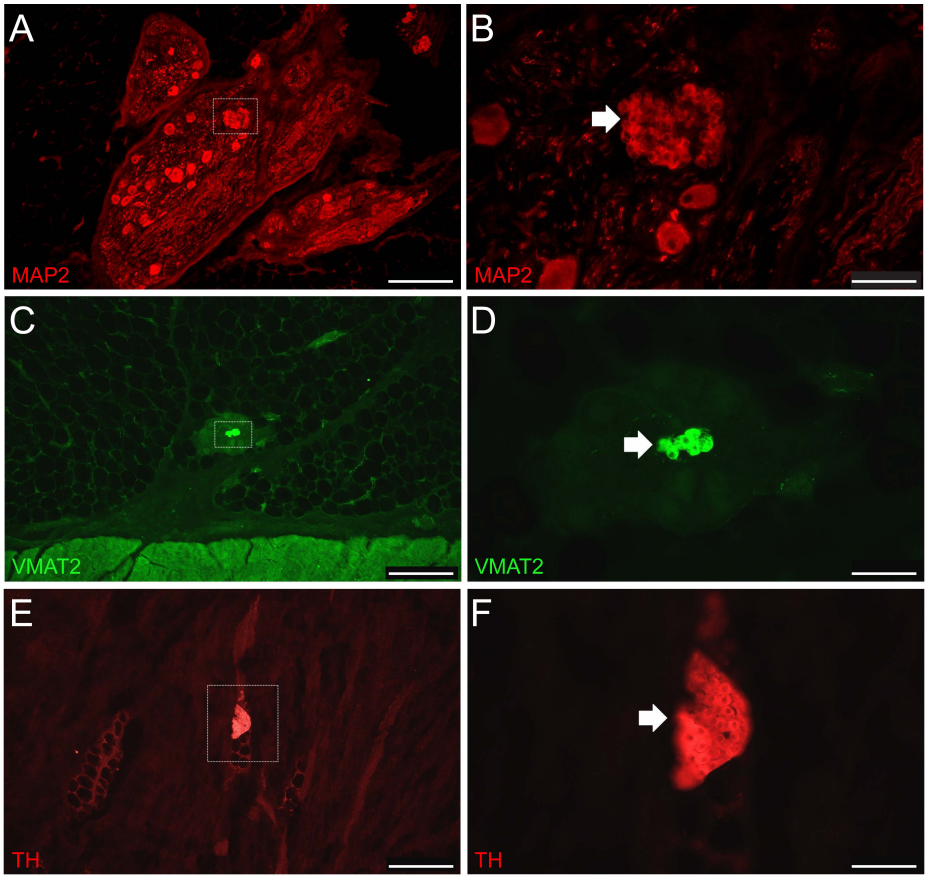

Online Figure III. Clusters of small intensely fluorescent (SIF) cells are found in the porcine right atrial ganglionated plexus (RAGP) fat pad. SIF cells were identified based on labeling for noradrenergic markers and MAP2 (microtubule-associated protein 2), their small size and frequent clustering. SIF cells were found at various sites throughout RAGP sections between neurons in the ganglia, in the atrial muscle and amongst fat cells. **A**, Low magnification fluorescence microscopic image of ganglia labeled for MAP2. **B**, Cluster of SIF cells shown at higher magnification. SIF cells (arrow) are much smaller than neurons in the same field. **C**, Low-magnification fluorescence microscopic image of small ganglion with SIF cells stained for VMAT2 (vesicular monoamine transporter 2). **D**, VMAT2-positive SIF cell cluster (arrow) at higher magnification. **E**, Cluster of SIF cells stained for TH (tyrosine hydroxylase) located between atrial muscle fibers. **F**, TH-positive SIF cell cluster (arrow) shown at higher magnification. Scale bars are 200 μm (**A, C, E**) and 50 μm (**B, D, F**).

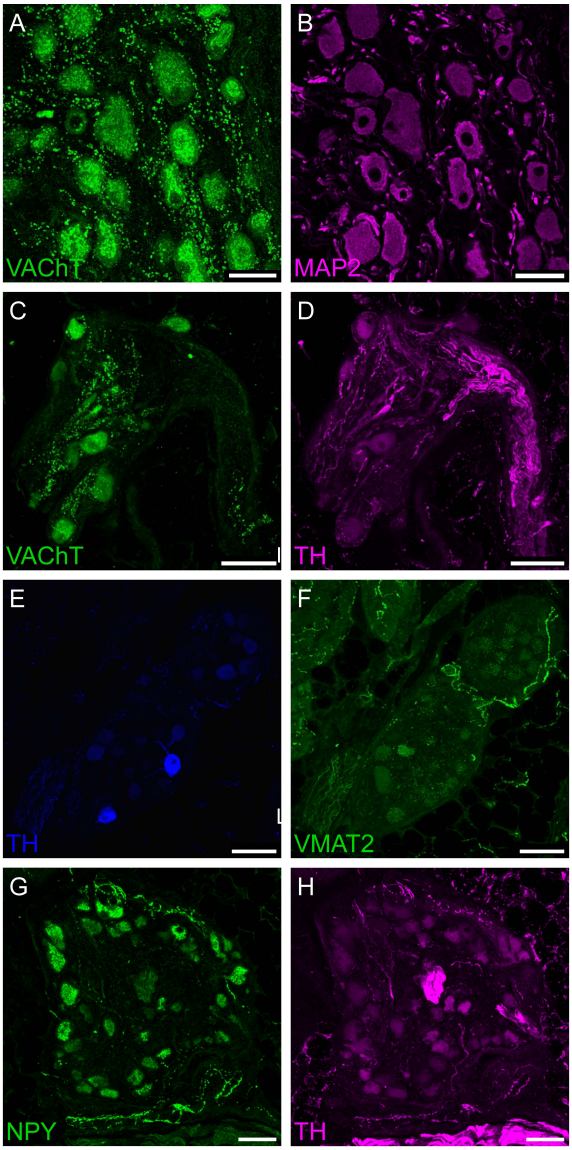

Online Figure IV. Neurochemical coding of the porcine right atrial gangliionated plexus (RAGP). Confocal images of ganglion double labeled for the cholinergic marker VAChT (vesicular acetylcholine transporter, **A**) and for MAP2 (microtubule-associated protein 2, **B**). Confocal images of ganglion double labeled for VAChT (**C**) and for noradrenergic marker TH (tyrosine hydroxylase, **D**) show that a few neurons contain both VAChT and TH. Confocal images of ganglia show that while some RAGP neurons stain for TH (**E**), they usually lack the essential noradrenergic marker VMAT2 (**F**), although positive staining for VMAT2 does occur in nerve fibers. Confocal images of a ganglion double labeled for NPY (neuropeptide Y, **G**) and TH (**H**) illustrate that many neurons contain NPY, but lack TH. In contrast, NPY and TH colocalized in some nerve fibers. Scale bars are 50 μm (**A-B**) and 100 μm (**C-H**).

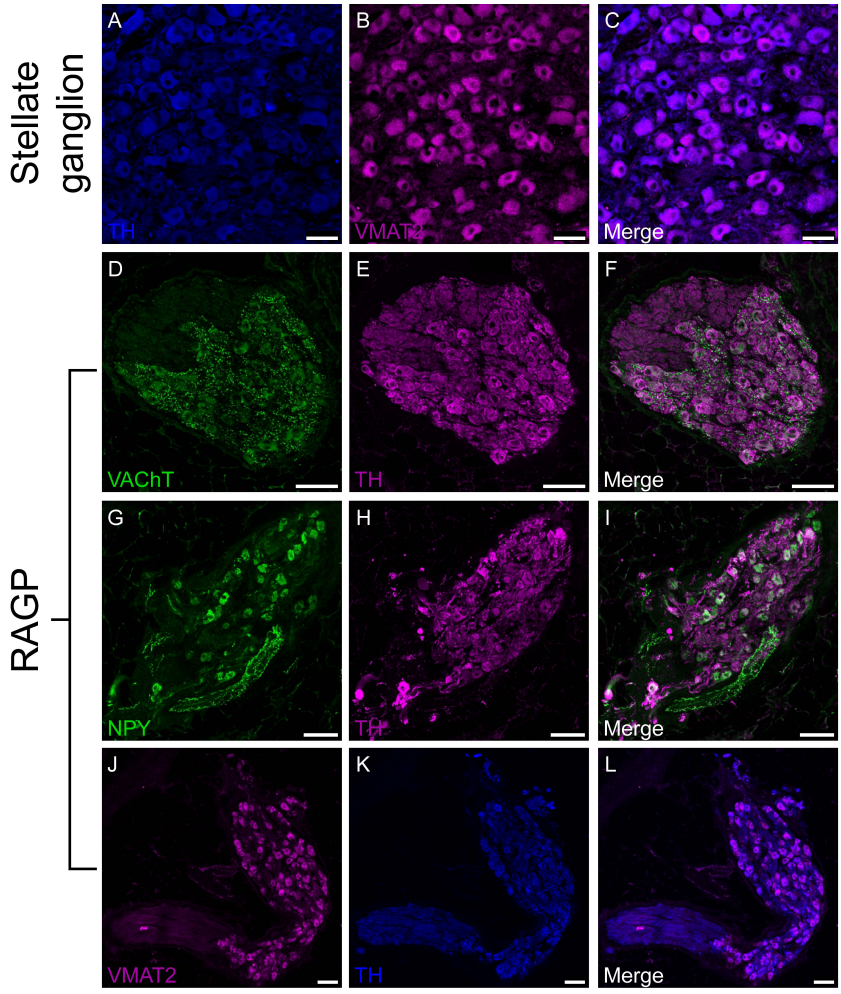

Online Figure V. Noradrenergic neurons in the stellate ganglia and atypical right atrial ganglionated plexus (RAGP) ganglion that contained noradrenergic neurons. A-C, Confocal images of double labeled section from porcine stellate ganglion showing that TH (tyrosine hydroxylase) and VMAT2 (vesicular monoamine transporter 2) are colocalized in noradrenergic neurons. **D-L**, Atypical RAGP ganglion that contained noradrenergic neurons. **D-F**, Confocal images of ganglion double labeled for VAChT (vesciular acetylcholine transporter, **D**) and TH (**E**) shows strong labeling of all neurons for TH. (**F**) Overlay image shows cholinergic varicosities around TH-positive neurons. **G-I**, Confocal images of the same ganglion double labeled for NPY (neuropeptide Y, **G**) and TH (**H**) shows many neurons labeled for each marker. (**I**) Merged image shows colocalization of NPY and TH in cell bodies. J-L Confocal images of same ganglion double labeled for VMAT2 (**J**) and TH (**K**). **L**, Merged image shows extensive colocalization of both markers in this ganglion. Scale bars are 50 μm (**A-C**) and 100 μm (**D-L**).

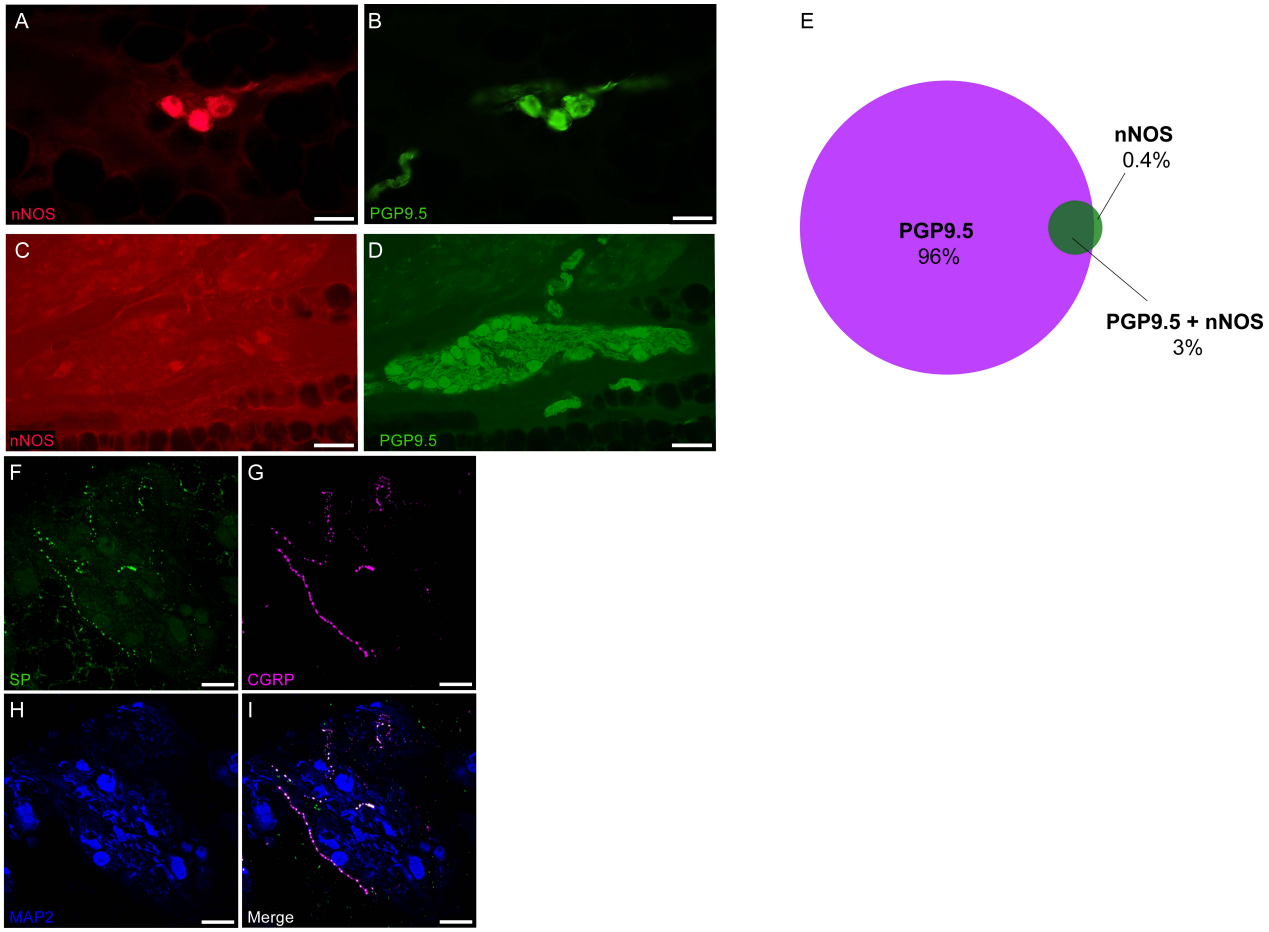

Online Figure VI. nNOS (neuronal nitric oxide synthase) is found in only a few neurons in the porcine RAGP and CGRP and SP are found in nerve fibers. **A-D**, Fluorescence microscopic images of sections double labeled for nNOS and PGP9.5 (protein gene product 9.5). **A-B**, Neurons that stain strongly for nNOS. **C-D**, Images from a typical ganglion that contains several PGP9.5-positive neurons that lack nNOS. **E**, Venn diagram illustrates proportion of PGP9.5-positive, nNOS-positive and both PGP9.5- and nNOS-positive neurons. **F-I**, CGRP (calcitonin gene-related peptide) and SP (substance P) are colocalized to varicose nerve fibers in porcine RAGP, but these do not surround ganglionic neurons. Confocal images of a ganglion that was triple labeled for SP, CGRP and MAP2 (microtubule-associated protein 2). **F-G**, Varicose nerve fibers staining for SP and CGRP, respectively. **H**, Staining for MAP2 shows neuronal cell bodies and their processes. **I**, Merged image shows the colocalization of SP and CGRP to nerve fibers and the close apposition of some nerve fibers to MAP2-positive neurons and processes. Neither SP nor CGRP is colocalized with MAP2. Scale bars are 50 μm (**A-B, F-I**) and 100 μm (**C-D**).

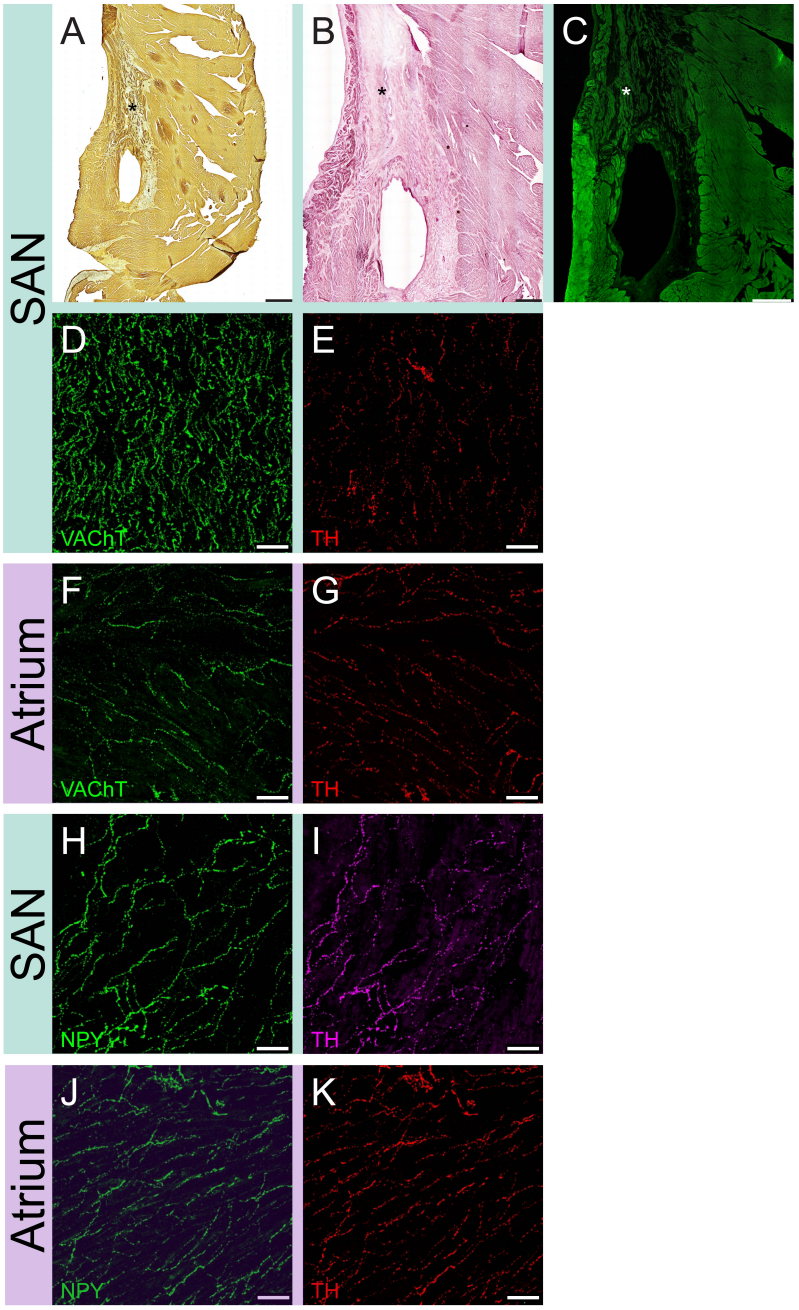

Online Figure VII. Differential cholinergic and noradrenergic innervation of the porcine sinoatrial node (SAN). A, Sections of SAN (*) from a female pig that underwent 3,3′-diaminobenzidine and HCN4 (hyperpolarization-activated cyclic nucleotide-gated channel 4; brown puncta) staining in the anatomic SAN region. H&E and connexin 43 staining of the working atrial myocardium border the region of the SAN region (*, **B**), which also demonstrates dense VAChT (vesicular acetylcholine transporter) staining (**C**). Sections of SAN (**D-E**) and right atrial myocardium (**F-G**) were double labeled for VAChT and TH (tyrosine hydroxylase). Confocal images from these sections show that while cholinergic nerves (**D**) are more abundant than noradrenergic nerves (**E**) in the SAN, both nerve types have similar density in atrial myocardium (**F-G**). Confocal images on the SAN and atrium myocardium stained for NPY (neuropeptide Y; **H, J**) and TH (**I, K**) showed colocalization. Scale bars are 2 mm (**A-C**) and 50 μm (**D-K**).

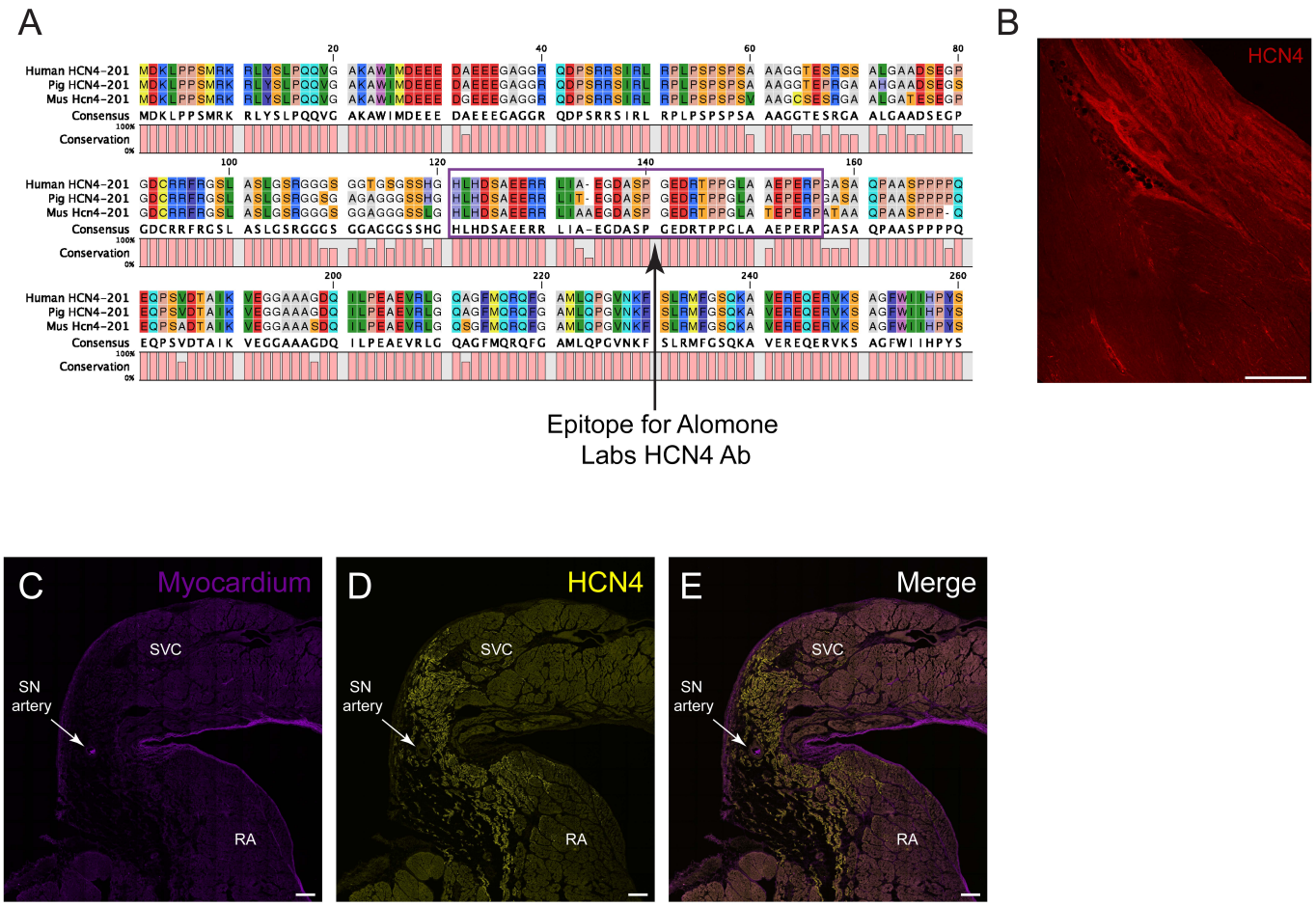

Online Figure VIII. Immunohistochemical and RNA in situ hybridization assessments of porcine SAN. A, Sequence homology comparing the *HCN4* gene in human, pig and mouse. Note that the human epitope used to generate the HCN4 antibody (Alomone labs, APC-052) is very similar to that of pig and mouse. **B**, Immunostaining of HCN4 in porcine SAN shows poor contrast. RNA in situ hybridization further confirmed *HCN4* gene expression (yellow) in the SAN region in a male pig (**C-E**). SN = sinus nodal; SVC = superior vena cava; RA = right atrium. Scale bars are 500 μm (**B**) and 200 μm (**C-E**).

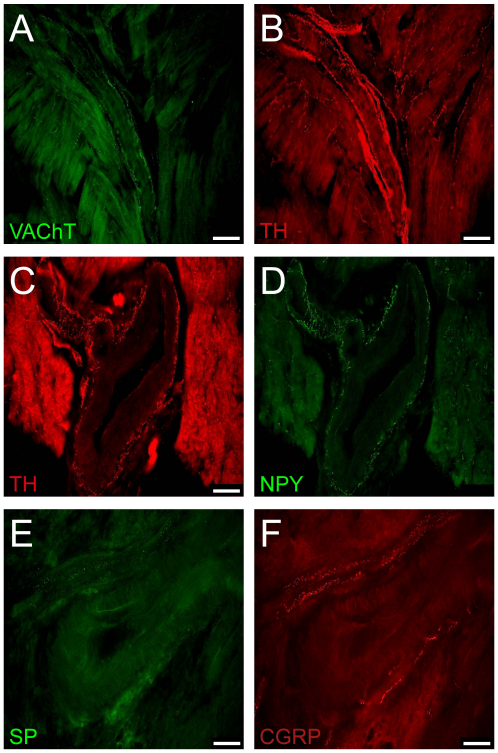

Online Figure IX. Atrial blood vessels are innervated by cholinergic, noradrenergic, and peptidergic nerve fibers. A-B, Double labeling for VAChT (vesicular acetylcholine transporter) and TH (tyrosine hydroxylase) shows cholinergic and noradrenergic nerves around vessel cut longitudinally. **C-D**, Double labeling for TH and NPY (neuropeptide Y) shows that these markers are colocalized around a blood vessel cut in cross section. **E-F**, Double labeling for SP (substance P) and CGRP (calcitonin gene-related peptide) shows that both sensory neuropeptides are present around a vessel cut in cross section, but CGRP is more abundant. Scale bars are 50 μm (**A-B**) and 100 μm (**C-F**).

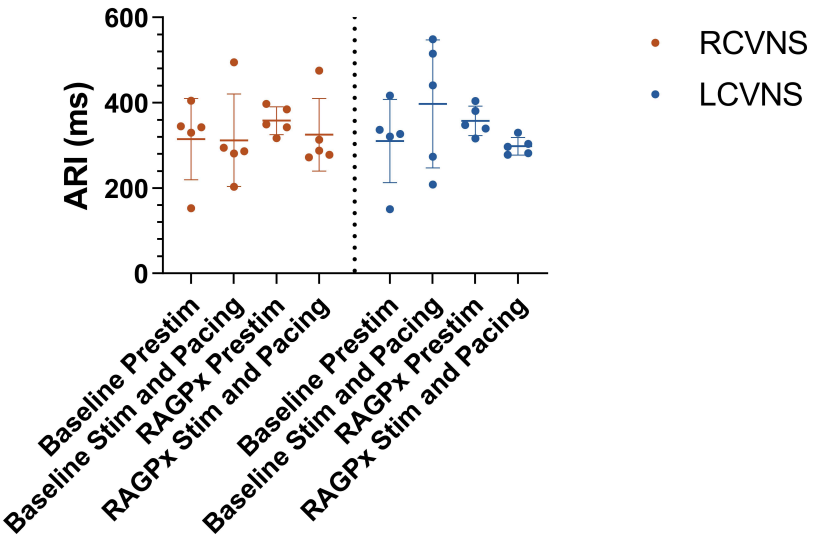

Online Figure X. Right atrial ganglionated plexus (RAGP) ablation did not impact vagal nerve stimulation (VNS)-induced changes in ventricular activation-recovery interval (ARI) during atrial pacing. No significant changes in average global ventricular ARI before and after RAGP ablation and before and during either right (RCVNS) or left cervical VNS (LCVNS) with concurrent atrial pacing were identified. Comparisons were made using repeated measures ANOVA. Prestim: prior to VNS; Stim: VNS; Pacing: atrial pacing; and RAGPx: RAGP ablation.

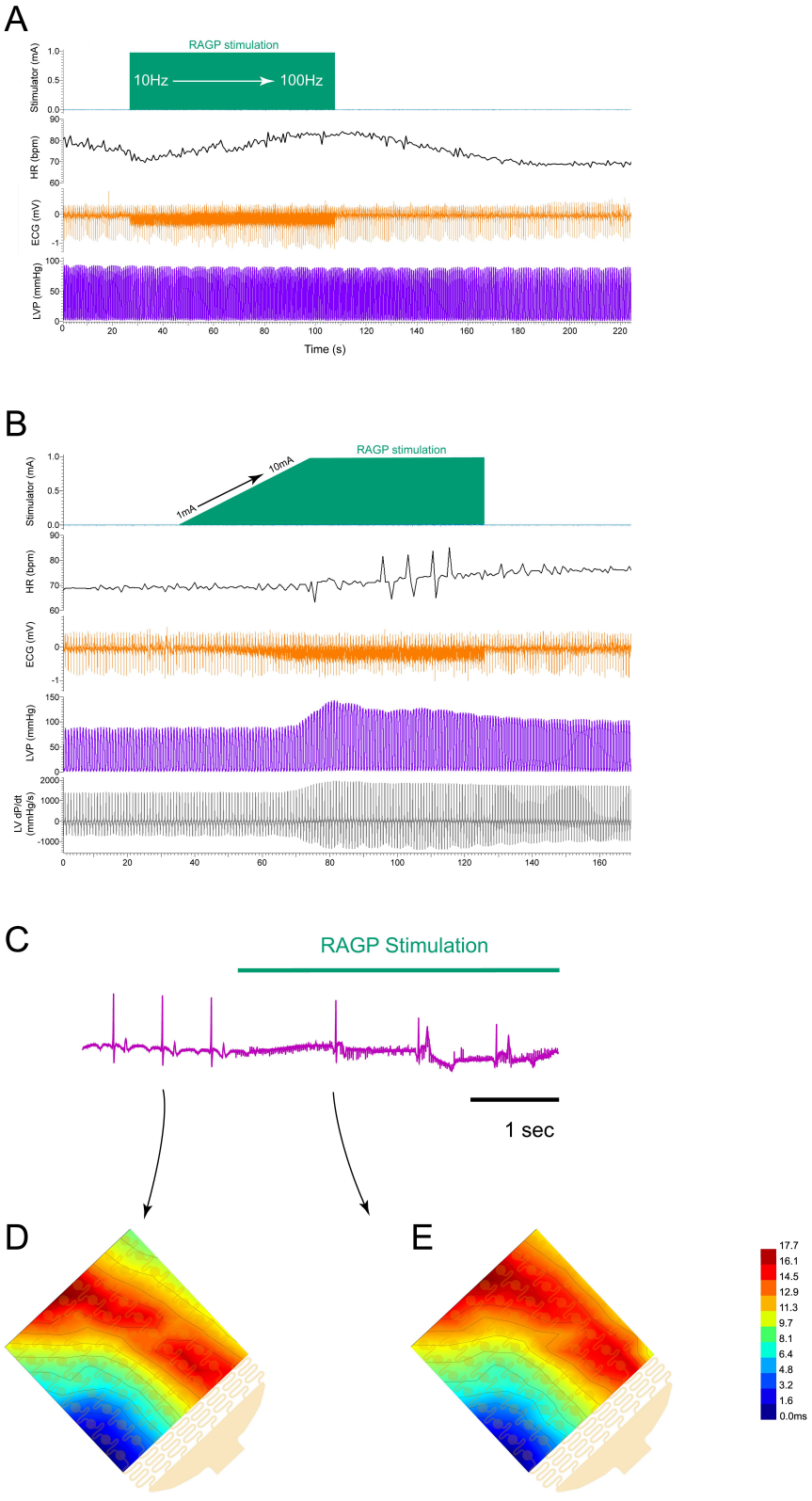

Online Figure XI. Stimulation of right atrial ganglionated plexus (RAGP) elicits different responses from the sinoatrial node (SAN) and left ventricle (LV). A, Example of bradycardia elicited by lower frequency (10 Hz) RAGP stimulation with tachycardia at higher frequency (100 Hz) stimulation. **B**, Increase in current from 1 to 10 mA with mild increase in HR and significant increase in LV pressure and contractility (dP/dt). **C**, Example of RAGP stimulation-induced bradycardia. Activation map before (**D**) and during (**E**) RAGP stimulation**.**

Online Video Legends

Online Video I. Network of ganglia and interconnecting nerve fibers are found in the porcine right atrial ganglionated plexus (RAGP). 3-dimensional projection of portion of immunolabeling-enabled three-Dimensional Imaging of Solvent-Cleared Organs (iDISCO+)-cleared porcine RAGP immunostained with PGP9.5 (protein gene product 9.5; purple).

Online Video II. 3-dimensional projection of ganglion found in porcine RAGP. iDISCO+-cleared ganglion immunostained with PGP9.5 (purple) at higher magnification.

Online Video III. Ganglia in the human RAGP are found within the adipose tissue and at the fat-muscle interface. 3-dimensional stack of sequential hematoxylin and eosin sections of human RAGP demonstrating ganglia embedded in fat as well as at the fat-posterior right atrial wall interface.

Online Video IV. Network of ganglia and interconnecting nerve fibers are found in the human RAGP. Portion of iDISCO+-cleared human RAGP immunostained with PGP9.5 (purple).

Online Video V. The sinoatrial nodal artery (SNA) supplies the human RAGP. MicroCT image sequence of contrast-injected right coronary artery (RCA; red) with sinoatrial nodal branch supplying the RAGP (yellow) of a human cadaveric cardiac specimen.

Online Video VI. The porcine sinoatrial node (SAN) is densely innervated. 3-dimensional projection of portion of porcine SAN immunostained with PGP9.5 (yellow). Muscle autofluorescence is purple. Note the multiple ganglia found in the SAN region.

Large nerve fibers can be seen along the crista terminalis. ST indicates sulcus terminalis; SVC, superior vena cava.